

Relevant features of the valley seismic response: the case study of Tuscan Northern Apennine sector

G. Vessia · S. Russo

Received: 5 July 2012 / Accepted: 28 April 2013 / Published online: 8 May 2013
© Springer Science+Business Media Dordrecht 2013

Abstract The so called “valley effect” relates to the typical seismic response of basin shaped bedrock filled by quaternary sediments. It is an aspect of the renowned “local seismic effect” that shall be taken into account when dealing with microzoning studies. Several experimental surveys and numerical simulations performed worldwide over the last 40 years, confirmed that valley responses under seismic excitations show common features in various geological contexts as far as the sedimentary valleys (e.g. alluvial and lacustrine plains), the intermountain valleys (e.g. alpine valleys) and graben shaped basins. Such features mainly depend on the basin geometry, referred to as the shape ratio SR, and the sediment and basin impedance contrast IC. Although researchers agree on the prominent role of local seismic effects for interpreting erratic damages caused by seismic shaking in urbanized areas, no fully shared strategies have been identified for taking into account valley effect within microzoning studies. In this paper, a numerical simulations on three models of trapezoidal shaped basins have been performed. These valley models relate to sediments and basins detected within the Tuscany Region territory during the VEL project. Results, in terms of the amplification index F_A have been provided. Three “valley effect charts” for various SR and IC values have been propose for taking into account the local seismic effects due to the basin amplifications within microzoning maps.

Keywords Valley effect · Local seismic effect · Impedance contrast · Shape ratio · Tuscan Apennine sector

G. Vessia (✉)
Department of Engineering and Geology, University “G. d’Annunzio” of Chieti-Pescara,
Via dei Vestini, 31, Chieti Scalo, Italy
e-mail: g.vessia@unich.it

G. Vessia
Institute of Research for Hydrogeological Protection, National Research Council, Bari, Italy

S. Russo
Polytechnic of Bari, Via Orabona, 4, Bari, Italy
e-mail: sarusso@poliba.it

1 Introduction

The “valley effect” is a well known local seismic phenomenon observed wherever basin shaped seismic bedrocks are filled by softer sediments. Several cities within Alpine and Apennine territories are set on these basins (e.g. Onna, Grenoble, Gubbio among others). This seismic effect is generally referred to the surface response and it is characterised by longer duration of time history signals than the inward wave train, amplified spectral ordinates at the centre and the edges of the valley and broader range of amplified periods/frequencies. Since [Bard and Bouchon \(1985\)](#) pioneering studies, the aforementioned features of “valley effects” have been described by means of the following variables:

- The shape ratio of the valley, SR, that is the ratio between the highest depth at the centre of the basin and the half of valley width;
- The bedrock–sediment impedance contrast, IC, defined as the ratio between the seismic impedance (that is ρV_s , where ρ is the density and V_s is the shear wave velocity) of the bedrock basin and the filling sediments.

Nonetheless, other aspects are relevant for valley seismic response although cumbersome to be generalized, that are:

- The non-linear behaviour of sediments overlying the basin;
- The sediment shear stiffness reduction and damping increasing with shear strain level;
- The frequency content of the strong motion input signal, its maximum amplitude and duration and their interaction with the basin amplified frequencies.

The present study focuses on seismic valley effects analysed by means of a numerical two-dimensional approach. One- and two-dimensional numerical analyses (1D and 2D, respectively) are commonly used to predict seismic local amplification effects. Three-dimensional analyses have been recently used to simulate basin effects by means of an accurate simulation of source mechanism and only simplified linear or viscoelastic behaviour of sediments ([Day et al. 2006](#); [Paolucci and Smerzini 2011](#)). These numerical studies can be used to draw seismic microzonation maps within urban centres by dividing municipalities into homogeneous response areas. The seismic response is characterized by amplification factors.

In the following, three “valley amplification charts” have been proposed depending on various SR and IC values measured within Tuscan territory. The three charts relate to three locations on the valley surface: the edge, the centre and the point in between. Such charts can be employed for microzonation maps of Tuscan municipalities placed on sediment filled basins and for those worldwide cases that can be compared to the Tuscan ones.

2 Local seismic effects on soil filled basins: past studies on induced amplifications

The first pioneering studies on the valley response have been addressed by means of theoretical and experimental approaches in the eighties ([Bard and Bouchon 1980a,b, 1985](#); [King and Tucker 1984](#); [Tucker and King 1984](#); [Silva 1988](#)) providing a general framework for studying common valley response characters by means of numerical simulations. According to the results of such studies, [Bard and Bouchon \(1980a,b, 1985\)](#) suggested to take into account 2D basin response whenever the shape ratio SR and the velocity contrast (that is the ratio between the sediment and the bedrock shear wave velocities) C_v , satisfy the following inequality:

$$SR > \frac{0.65}{\sqrt{C_v - 1}} \quad (1)$$

Accordingly, truly valley effects take place when SR is higher than 0.2 for high IC values ($IC = 7$) whereas for high SR values $SR > 0.8$ when IC is higher than 2. However, contemporary observations show that 2D valley amplifications still play a role when shallow basins are considered (King and Tucker 1984; Bielak et al. 1999; Makra et al. 2005, among others). These cases relate to shape ratios $SR < 0.2$ and basin geometry far from a flat shape. Since the first experiences, several case studies have been investigated worldwide for detecting and quantifying valley effects where urban centres were placed on basin shaped bedrocks filled by softer quaternary sediments in seismic areas: e.g. the valley near Fujisawa City (Psarropoulos and Gazetas 2007; Gelagoti et al. 2007), Gubbio valley (Castro et al. 2004; Luzi et al. 2005), Riva del Garda valley (Faccioli and Vanini 2003), Adige Valley (Faccioli and Vanini 2003; Paolucci 1999), Val di Sole (Faccioli and Vanini 2003; Delgado et al. 2001), Rhone valley (Roten et al. 2004), San Giuliano di Puglia (Lanzo and Pagliaroli 2009; Puglia et al. 2009), Marina district valley (Zhang and Papageorgiou 1996), Kirovakan valley (Bielak et al. 1999), Kefalonia valley (Gazetas 1997; Chávez-García and Faccioli 2000), Mygdonian basin (Chávez-García and Faccioli 2000; Makra et al. 2005), Tarcento valley (Cauzzi et al. 2010) and Castelnuovo Garfagnana valley (Russo et al. 2008).

Furthermore, in the last ten years, two European research projects investigated the seismic valley response: (1) the project EUROSEIS-RISK, funded by the research Department of the European Commission, within the context of the Environment Programme “Global Change and Natural Disasters”. It was developed from 2001 to 2005 to assess seismic hazard, site effects and soil-structure interaction within a site test placed within the Mygdonian graben, in the north of Greece, 35 km far from Thessaloniki: it is known as Euroseist valley test; (2) the project named SISMOVALP “Seismic hazard and alpine valley response analyses” (<http://www.risknat.org/projets/sismovalp/CD2/Partners.html>) within the European project INTERREG III B 2003–2006, which outlined common geometric, material and behaviour features of the intermountain valleys such as the following alpine valleys: Isère river valley, Grenoble (France); Tagliamento river valley, Tolmezzo (Italy); Alluvial fan valley, Gemona (Italy); Resia Valley, Stolvizza (Italy); Fluvial fan valley, La Salle (Italy); Val Pellice Valley, Torre Pellice (Italy); Upper Soka valley, Bovec (Slovenia); Rhone valley, Valais (Switzerland).

Both the above mentioned projects dealt also with 2D numerical simulations of free field valley responses and their relevant features were expressed in terms of SR and IC: for the Euroseist valley, the phenomenon of the energy trapping and the incoming wave focusing toward the surface at the valley center is confirmed, although only IC seems to control the amplification magnitude where irregular basin shapes are considered (Faccioli and Vanini 1998; Makra et al. 2005; Vanini et al. 2007). As the Alpine valleys are concerned, the basins can be sketched as sine-shaped ones although real symmetric and asymmetric shapes are detected depending on the mechanical properties of basin sides and their origin: the V shape mostly relates to fluvial or glacial erosion process whereas the U shape to extensional tectonics genesis. Similarly to the results of SEISM-RISK project, the SISMOVALP investigated several valleys with different SR and IC values confirming the need of extending the 2D behavior of the shallow valley ($SR < 0.2$), indeed. This means that although the shape ratio is the common way to refer to the basin geometry, it is seldom not able to describe the seismic amplification effects of the irregular shaped basins.

Recently, some researchers proposed to introduce the amplifications induced by the “seismic valley effects” within the building codes by modifying the design spectra by means of different strategies (Chávez-García and Faccioli 2000; Faccioli and Vanini 2003; Cauzzi et al. 2010; Russo et al. 2008; Vessia et al. 2011). They all isolated the “valley effect” by calcu-

lating the ratio between 2D and 1D acceleration spectra at the valley surface and suggested different amplification values calculated at the centre and at the edges of the valleys.

In the present paper, the authors performed a numerical simulation campaign aimed at calculating the amplification valley effect for microzoning studies. Seismic microzoning aims at identifying those areas with homogeneous seismic response, in terms of amplification factors, for urban planning purposes. Such studies are needed within those territories exposed to high seismic hazard. Microzonation maps are used for supporting the planning decisions and recognising the best areas where setting the emergency camps after strong earthquakes occurrence. In this respect, real SR and IC values have been used within the present numerical simulations carried out by means of trapezoidal shaped valley models. These simulations relate to real intermountain valleys filled by sediments detected within the Northern Apennine sector, in the Tuscany Region territory. As a matter of fact, from 1998 to 2004, the Tuscany Region Office for Seismic Risk Prevention supported the Italian pioneering project named VEL (Local Effect Evaluation) to address microzoning studies at urban scale within the most seismically hazardous regional territories. The present authors were involved in it as well as many Italian researchers from several universities and research offices. Some project outcomes as in field and laboratory tests, are available for free at the website: http://www.regione.toscana.it/banchedati/index.html_1186952989.html.

Accordingly, hereafter, at first the common characters of the Tuscan valleys will be illustrated with respect to the geological context, their geometric features and the filling sediment properties derived by several laboratory (sieve analyses, resonant column tests, triaxial tests) and in field investigations (down hole tests, refraction and reflection tests).

3 Tuscan valleys within the Northern Apennine sector: geological and seismological features

Sedimentary valleys can be detected within several provinces of Tuscany Region, such as Lucca, Firenze, Massa-Carrara and Arezzo (Fig. 1a). The northernmost basins are oriented NW-SE (Mugello, upper Valdarno, Aulla-Olivola) and the others from NNW to SSE, according to a belt parallel to the northern Apennine arc (e.g. Val di Chiana, Alta Valtiberina). They are intermountain valleys originated by the extensional tectonics within the Northern Apennine sector and then filled by fluvial-lacustrine sediments during the Late Pliocene–Early Pleistocene (Bossio et al. 1993; Martini and Sagri 1993) (Fig. 2). Such basins are mainly considered half-grabens or asymmetric grabens, bounded by W and SW dipping master faults (e.g. Mugello) or by ENE dipping faults (Alta Valtiberina, Upper Valdarno, Val di Chiana) (Barchi et al. 2001). Since the latest Early Pleistocene–Middle Pleistocene the entire area within the Northern Apennine margin was subjected to the regional uplift (Bartolini 2001) which forced the integration of the modern fluvial systems and exerted a major control on alternating phases of fluvial-lacustrine aggradation and degradation. During the uplift phase, the sedimentation was represented by terraced fluvial gravels and sands and lacustrine travertines, also climatically (Mugello, Val di Chiana, Alta Valtiberina) and eustatically controlled (e.g. Lower Valdarno) (see Fig. 3).

The sedimentary sequence of Garfagnana and Lunigiana areas are characterized by Plio-Pleistocene fluvio-lacustrine soils within the basin of Barga-Castelnuovo and Aulla-Olivola dated in Villafranchian age (Fig. 3). Such soils are made up of clayey–sandy units including coarser levels at the bottom and upon it, gravel cemented soils interbedded with conglomerates, sands and silts. Several orders of fluvial terraces cover the fluvio–lacustrine deposits

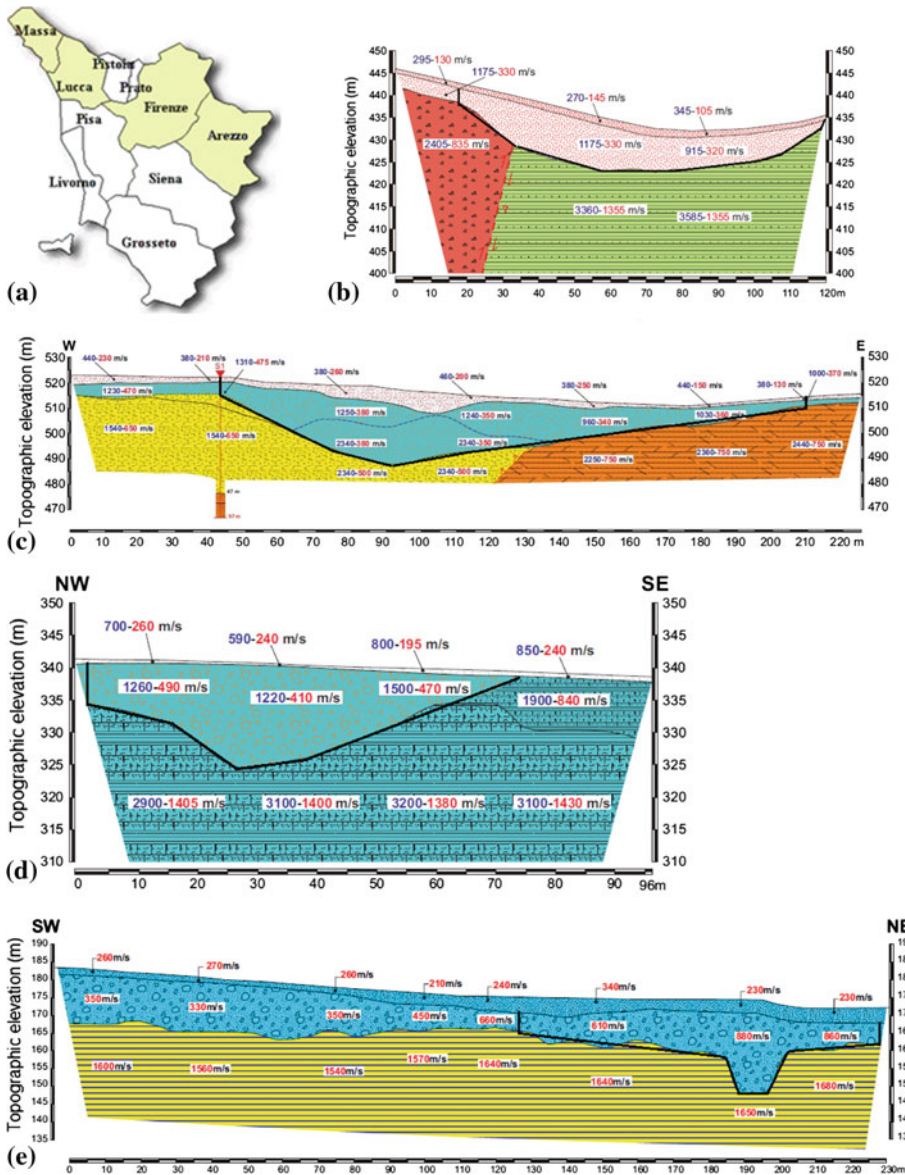


Fig. 1 a Tuscany Provinces where alluvial valleys are located; Valley examples at b Firenzuola (FI) c Castiglione di Garfagnana (LU), d Fivizzano (MS), e Galliciano (LU)

dated to superior Olocene–Pleistocene age of Serchio river, Magra river and its tributaries (D’Amato et al. 1986).

Figures 1b–e show some examples of urbanized basins detected by refraction tests (indirect seismic testing method) and then litho–technical characterized by means of direct soundings, continuous coring and laboratory tests on undisturbed samples.

As seismic hazard is concerned, almost all the Italian territory can be considered affected by tectonic activity. The present tectonics (that is Quaternary tectonics) with $M > 6$ earth-

Fig. 2 Main Northern Apennine intramountain basins. B: inner margin of the Northern Apennines: 8) Aulla-Olivola; 9) Lower Valdarno; 10) Firenze-Pistoia; 11) Mugello; 12) Upper Valdarno; 13) Val di Chiana; 14) Upper Valtiberina; 15) Tavernelle–Pietrafitta; 16) Gubbio; 17) Colfiorito; 18) Tiberino; 19) Paglia–Tevere Graben; 20) Roman basins; 21) Rieti; 22) Leonessa (After Bosi et al. 2004, modified)

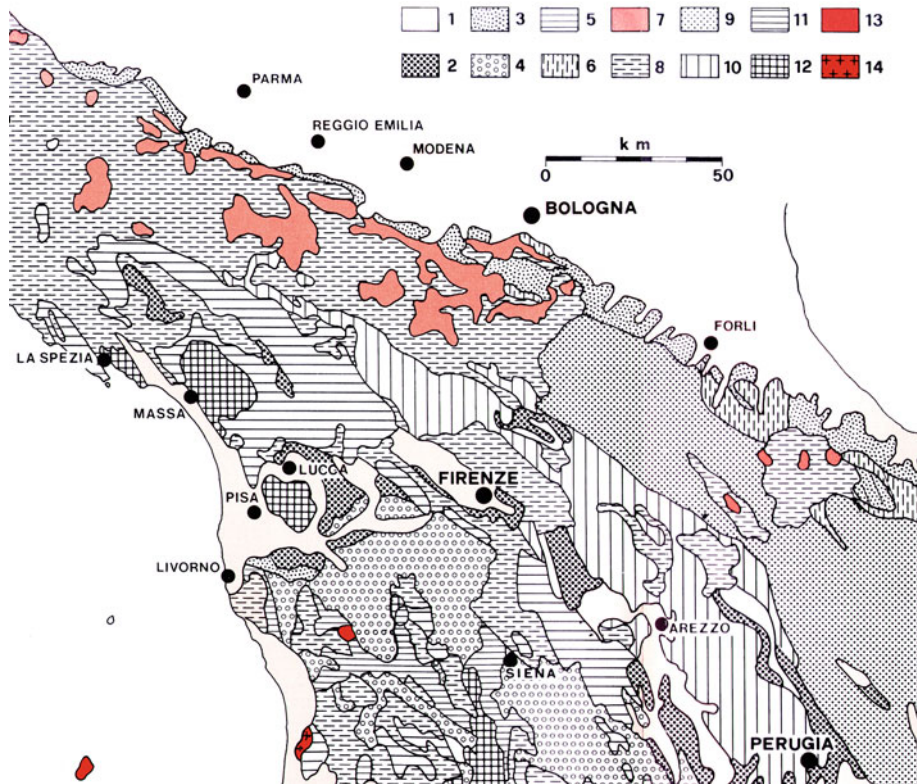


Fig. 3 Geologic map of Tuscan–Emilian Apennine. (1) Continental and marine deposits (upper Pleistocene–Olocene). (2) Fluvial-lacustrine deposits (Middle Pliocene–Middle Pleistocene). (3) Soil mainly marine deposits (Lower Pliocene–Lower Pleistocene). (4) Marine soil deposits belonging to Tyrrhenian side (Pliocene). (5) Lacustrine and marine deposits with Tyrrhenian evaporate (Messinian, lower Pliocene). (6) gypsic–sulphides formation belonging to the Po side. (Messinian). (7) Epi–Iugurian units (Upper Eocene–Miocene). (8) Ligurian units (Jurassic Oligocene). (9) Umbra–Romagna units and Adriatic–Marches units (Upper Triassic, Upper Miocene) (10) Cervarola Falterona units (upper Cretaceous, middle Miocene) (11) Tuscan Nappe. (Upper Triassic, lower Miocene). (12) Tuscan Metamorphic Complex (Triassic, upper Oligocene). (13) Extrusive igneous rocks (Miocene–Olocene) (14) Intrusive igneous rocks (Miocene–Pliocene). (After AAVV (2004) modified)

quakes, affects the Apennine chain, the Calabria region, the eastern Sicily and the central-eastern Alps (Gruppo di lavoro CPTI 2004). It is conditioned by the most recent evolution of the Alpine and Apennine orogenesis according to the tectonic history of the different Italian structural domains. The Northern Apennine, studied hereafter, belongs to a sector that was affected by uplift and normal faulting during the Quaternary (CNR-PFG 1987). Normal faults in the Northern Apennines have been responsible for the formation of graben basins such as the Garfagnana, Mugello and Casentino intramountain depressions (Moretti 1992; Meletti et al. 1993; Benvenuti 1995). All the faults bordering the mentioned basins are characterized by geomorphic features referring to the Quaternary activity (generally known as the tectonically controlled continental deposition).

A recent study of the seismotectonic framework of the Northern Apennine sector has been undertaken with the contribution of the Tuscany regional office for the Seismic risk prevention and the University of Siena (Mantovani et al. 2011). Table 1 shows the comprehensive catalogue of strong motion events (Magnitude higher than 5) occurred within the Tuscan Northern Apennine sector after the year 1000 BC. (Mantovani et al. 2011).

As can be seen, the Magnitude values range between 5.1 and 6.5, although higher number of earthquakes occurred in the Apennine sector of the Region with the hypocentral depth ranging between 5 and 10 km. In particular, Garfagnana and Lunigiana basins and the Upper Valtiberina are affected by a seismic activity registered downward to 20 km depth.

As the hazard seismic zonation is concerned, according to the Regional Resolution n. 841 of 26.11.2007, referred to as Del. GRT 841/07, the municipalities related to the considered valleys belong to the seismic zone 2, meaning that the maximum expected horizontal acceleration on the rigid ground (seismic soil class A, with a mean velocity over 30 m depth is $V_{s30} \geq 800 \text{ m/s}$) is 0.25 g, according to the seismic hazard zonation based on 475 years return period as reported in Table 2. This Table shows that Tuscan basins suffer similar maximum ground accelerations although the expected one varies between 0.15 and 0.22 g. Nevertheless, in this study, the maximum acceleration 0.25 g has been considered as the reference ground acceleration.

4 Litho-technical features of the considered Tuscan valleys

The studied valleys (Fig. 1b–e) have been described in terms of geometric shapes and measured velocities of both the basin bedrock and the sediments. The real geometry of the valleys are asymmetric, triangular shaped with maximum depth of 10–30 m and lateral extensions ranging between 40 and 170 m. The basins are commonly filled by two strata of alluvial soils: from the bottom upwards there are stiffer sediments with higher wave velocity under a few meter softer upper stratum with lower wave velocity. Table 3 summarizes geometrical features of the studied valleys in terms of SR. As can be seen, SR values range between 0.16 and 0.87, meaning that Tuscan valleys vary between shallow to deep ones. Moreover, in columns 4 and 5, mean values of the shear wave velocities V_{sm} relating to the sediments and the bedrock, respectively, for each basin cases are listed. As can be seen, V_S values related to bedrocks are, in some cases, less than 800 m/s. According to the European building code Eurocode 8 (EC8) (CEN 2003), seismic bedrock is considered for $V_S \geq 800 \text{ m/s}$. On the contrary, the sediments V_S mean values over 30 m depths are quite high, mostly corresponding to B seismic soil categories, although such circumstance is variable point to point depending on the thickness of softer surficial deposits. Thus, based on V_{s30} , sediments shear wave velocity can be assumed to vary from C to B seismic soil categories. Consequently, the velocity contrasts between the bedrock and the overlaying sediments are quite low. Column 6 in Table 3 shows

Table 1 $M > 5$ earthquake list occurred within the Tuscan northern Apennine sector after the year 1000 (after CPTI04).

Year	Month	Day	Epicentral zone	Latitude (°N)	Longitude (°E)	Magnitude (M)	Intensity (Imax)	T (year)
1005			Arezzo	43,463	11,879	5,4	7–8	
1117	3	1	Toscana Nord Ovest	44,08	10,45	5,2G	8	112,2
1148			Firenze	43,777	11,249	5,2	7	30,8
1270			Sansepolcro	43,57	12,141	5,4	7–8	122
1293	7	11	Pistoia	43,932	10,913	5,6	8	23,6
1320	12	16	Siena	43,321	11,328	5,2	7	27,4
1352	12	25	Monterchi	43,465	12,127	6	9	32
1353	1	1	Sansepolcro	43,57	12,133	6,0G	9	0
1414	8	3	Toscana settentrionale	43,933	10,6	5,2G	7	61,6
1414	8	7	Toscana occidentale	43,271	11,12	5,7	7–8	0
1453	9	28	Firenze	43,77	11,3	5,3	8	39,1
1470	4	11	App. Bolognese	44,161	11,037	5,2	8	16,5
1481	5	7	Lunigiana	44,276	10,13	5,8	8–9	11,1
1489			Sansepolcro	43,57	12,141	5,2	7	7,6
1497	3	3	Lunigiana	44,25	9,92	5,9G	9	8,3
1527	10	4	Pistoia	43,932	10,913	5,4	7–8	30,6
1542	6	13	Mugello	44	11,38	5,9	9	14,7
1559	4	11	Sansepolcro	42,62	12,19	5,3M	7	16,8
1597	8	3	Mugello	43,98	11,43	5,2	7–8	38,3
1600			Palazzuolo	44,113	11,548	5,4	7–8	2,3
1611	9	8	Scarperia	44,02	11,37	5,1	7–8	11,8
1646	4	5	Livorno	43,55	10,321	5,2	7	34,6
1694	4	8	Sansepolcro	43,57	12,141	5,1	7	48
1724	12	11	Travale	43,202	11,017	5,3	7–8	30,7
1731	3	29	P. Santo Stefano	43,67	12,04	5,5M	7–8	6,3
1740	3	6	Garfagnana	44,124	10,59	5,2	7–8	8,9
1741	10	1	Siena	43,321	11,328	5,2	7	1,6
1742	1	27	Livorno	43,55	10,32	5,2	7	0,3
1762	4	15	Borgo S.Lorenzo	44	11,333	5,2	7	20,2
1767	1	21	Fivizzano	44,18	10,11	5,1	7–8	4,8
1777	10	5	Radicofani	42,88	11,756	5,4	8	10,7
1796	2	5	Aretino	43,533	11,872	5,1	7	18,3
1798	5	26	Siena	43,342	11,416	5,2	7	2,3
1804	10	18	Tegonia	43,333	11,083	5,2	7	6,4
1812	9	11	Val Di Pesa	43,665	11,135	5,4	7–8	7,9
1814	4	3	Livorno	43,633	10,361	5,2	6–7	1,6
1834	2	14	Alta Lunigiana	44,449	9,859	5,6	8–9	19,9
1834	7	4	Alta Lunigiana	44,439	10,021	5,1	6–7	0,4
1835	2	6	Borgo S. Lorenzo	43,933	11,383	5,2	7	0,6
1837	4	11	Alpi Apuane	44,174	10,181	5,7	10	2,2
1843	10	25	Vernio	44,072	11,144	5,2	7–8	6,5

Table 1 continued

Year	Month	Day	Epicentral zone	Latitude (°N)	Longitude (°E)	Magnitude (M)	Intensity (Imax)	T (year)
1846	8	14	Orciano Pisano	43,531	10,5	5,7	9	2,8
1864	12	11	Mugello	44,042	11,282	5,1	7	18,3
1869	2	7	Siena	43,333	11,333	5,2	7	4,2
1869	9	26	San Gimignano	43,495	11,077	5,2	7	0,6
1871	7	29	Guardistallo	43,301	10,619	5,1	7–8	1,8
1871	10	22	Radda	43,417	11,333	5,2	7	0,2
1895	5	18	Impruneta	43,75	11,25	5,2	7	23,6
1899	6	26	Valle del Bisenzio	43,9	11,12	5,1	7	4,1
1902	3	5	Garfagnana	44,093	10,463	5,2	7	2,7
1902	8	4	Fivizzano	44,2	10,2	5,2	7	0,4
1903	7	27	Lunigiana	44,329	9,953	5,2	7–8	1
1904	11	17	Pistoiese	43,964	10,82	5,2	7	1,3
1907	12	20	Radda	43,483	11,367	5,2	7	3,1
1909	8	25	Murlo	43,15	11,403	5,4	7–8	1,7
1911	9	13	Chianti	43,399	11,332	5,1	7–8	2
1914	10	27	Garfagnana	43,911	10,598	5,8	7	3,1
1917	4	26	Monterchi	43,465	12,125	5,8	9–10	2,5
1919	6	29	Mugello	43,95	11,48	6,2	9	2,2
1919	9	10	Piancastagnaio	42,793	11,788	5,4	8	0,2
1919	10	25	Monterchi	43,57	12,132	5,2	6	0,1
1920	9	7	Garfagnana	44,18	10,28	6,5	10	0,9
1929	7	18	Mugello	43,988	11,507	5,1	7	8,9
1930	5	24	Fiumalbo	44,136	10,724	5,2	6	0,9
1931	9	5	Firenzuola	44,057	11,367	5,1	7	1,3
1939	2	11	Marradi	44,002	11,431	5,2	7	7,4
1939	10	15	Garfagnana	44,119	10,255	5,2	7	0,7
1940	10	16	Radicefani	42,885	11,867	5,3	7–8	1
1948	6	13	Sansepolcro	43,536	12,104	5,2	7–8	7,7
1950	4	1	Rosignano M.	43,477	10,521	5,1	7	1,8

The M values are the mean value among different scale of Magnitude used within the CPTI04 to classify the energy of the earthquake, according to the description provided within the CPTI04. The letters G and M after the Magnitude values (Magnitude column) stand for the initials of the authors that suggested those values: G refers to [Guidoboni and Comastri \(2005\)](#) and M to [Mariotti and Guidoboni \(2006\)](#). T is the time interval between two neighboring seismic events over the list, e.g. the current and the previous one

C_v values ranging between 1.48 and 3.70. Accordingly, the impedance contrast IC values for the cases studied range between 1.22 and 6.7. These values, are then considered within the numerical analysis, in terms of SR and IC. For SR index three values have been considered, 0.2, 0.4 and 0.8 that are representative for three valley types: shallow, deep and very deep. Five IC values have been considered representing the range 1.2–6.7. Finally, the groundwater presence within the valley models was actually not taken into account in although wet conditions of the sediments have been considered by means of their physical properties.

Table 2 Seismic zonation of Tuscan municipalities where sediment filled valleys are detected

Municipality	Seismic zones (Del. GRT 841/07)	a_g (DM 14 gennaio 2008) [g]
Castiglione di Garfagnana (LU)	2	0.204
Firenze (FI)	2	0.201
Fivizzano (MS)	2	0.200
Fosdinovo (MS)	2	0.152
Galliciano (LU)	2	0.193
Minucciano (LU)	2	0.195
Molazzana (LU)	2	0.194
Pieve Santo Stefano (AR)	2	0.217
Castel San Niccolò (AR)	2	0.160
Villa Collemandina (LU)	2	0.204

Table 3 Main geometrical and dynamic characters of the Tuscan intermountain valleys, according to SR and C_v parameters: h = height of the sediment at the center of the valley; C_v = velocity contrast between the bedrock and the sediment shear wave velocities; V_{sm} = mean value of shear wave velocity of the sediments calculated along the maximum depth of the basins; SR = shape ratio of the valley

Site	h (m)	SR	V_{sm} (m/s)		C_v ($V_{Sbedrock}/V_{Ssediment}$)
			bedrock	sediment	
Castiglione G. (LU)	30	0.34	630	360	1.75
Firenze (FI)	10	0.20	1,200	325	3.70
Fivizzano (MS)	17	0.37	1,400	450	3.11
Galliciano (MS)	26	0.79	1,390	450	3.10
Minucciano (LU)	12	0.55	1,150	590	1.95
Minucciano (LU)	8	0.53	1,130	700	1.61
Molazzana (LU)	13	0.87	970	425	2.28
Pieve S. Stefano (AR)	8	0.16	525	355	1.48
S. Niccolò (AR)	14	0.48	1,455	705	2.06
Villa Collemandina (LU)	11	0.42	1,300	585	2.22

5 2D numerical analyses for the basin amplification prediction

1D and 2D numerical simulations have been undertaken by [Vessia et al. \(2011\)](#) within Tuscan basins for pointing out the role played by the basin geometry, the topography and the sediment seismic behaviour in Tuscan territories. The results showed the distribution of 2D amplifications throughout the basin width is able to explain local differences in provoked damages. On the contrary, 1D numerical simulations take into account local variation in soil layer impedance contrast and thickness but cannot be used where basins and complex buried geological settings are detected. Hence, the present 2D numerical analyses have been carried out for deriving amplification factors due to seismic “valley effects” for Tuscan territory conditions, such as seismic hazard level, geometric characters and soil mechanical properties. Due to the structure of the considered basins, they are elongated to one direction; this means that the symmetry plane is verified for 2D analysis meaningfulness. 3D analyses are

Table 4 Parameters of numerical analyses: density [kg/m^3] (*italic*) and shear wave velocities [m/s] (**bold italic**) of the fifteen valley models studied, according to SR and IC values

IC	SR				
	1.22	1.90	2.65	4.44	6.17
0.2	<i>2,100</i> 780	<i>2,100</i> 500	<i>2,100</i> 360	<i>1,800</i> 250	<i>1,800</i> 180
0.4	<i>2,100</i> 780	<i>2,100</i> 500	<i>2,100</i> 360	<i>1,800</i> 250	<i>1,800</i> 180
0.8	<i>2,100</i> 780	<i>2,100</i> 500	<i>2,100</i> 360	<i>1,800</i> 250	<i>1,800</i> 180

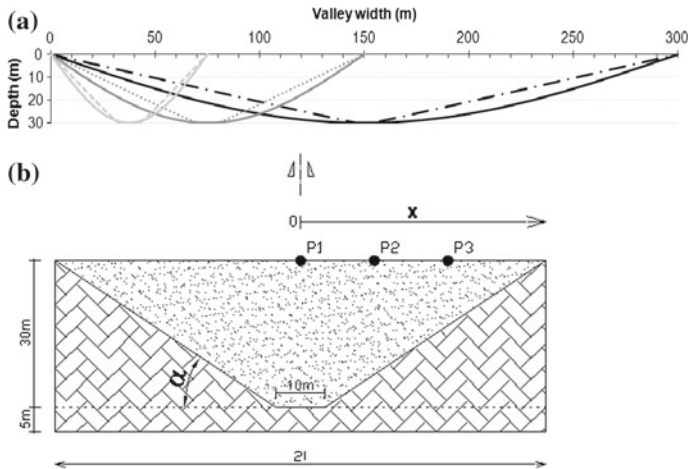


Fig. 4 **a** Sketches of the valley models used for numerical simulations of the Tuscan real valleys: SR = 0.2 in black; SR = 0.4 in grey; SR = 0.8 in light grey; **b** valley model used for numerical analysis: P1 ($x/l = 0$), P2 ($x = 0.31l$) and P3 ($x = 0.61l$) are the surface locations where 2D seismic response has been calculated

not attempted because they are not able to accurately describe the non-linear seismic behaviour of surficial sediments (Paolucci and Smerzini 2011). It is well known that local seismic responses are strongly affected by: (1) input motion amplitude and frequency content; (2) local geological and geomorphological settings and (3) non-linear properties of surficial sediments, their thickness and geometric arrangements. Thus, the results of this study can be methodologically used within other territories. However, the outcomes of this study can be used in Tuscany and wherever similar seismic, geological and geotechnical conditions can be found. The aforementioned Tuscan conditions have been grouped by three generalized geometric cases, based on three shape ratios SR and five material types classified by means of the impedance ratio IC values as shown in Table 4. Furthermore, the real triangular shape with the vertex at the bottom represents a numerical singularity for numerical simulation. Thereby, for the present numerical analyses trapezoidal shapes have been used as shown in Fig. 4a, b. This is the most representative regular shape for Tuscan irregular valley geometry; the base on the bottom is assumed equal to 10m according to a benchmark study on the influence of the base dimension on the surficial response of the models.

Numerical analyses have been performed on three valley models, from shallow (SR = 0.2) to deep and very deep valley (SR = 0.4 and 0.8), and for five IC values (IC = 1.22, 1.90, 2.65, 4.44, 6.17) according to the assumption of constant soil properties for the sediments

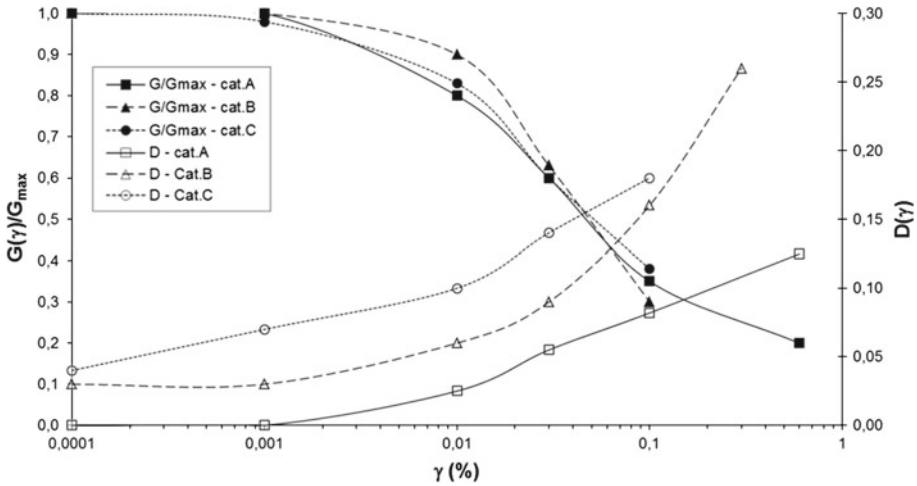


Fig. 5 $D(\gamma)$ and $G(\gamma)/G_{max}$ measured curves on Tuscan sediments for dynamic equivalent linear numerical analyses

over 30 m depth. Seismic soil categories considered for the sediments, are B and C according to EC 8. Moreover, IC values have been calculated by dividing five sediment V_s values (that are 780, 500, 360, 250 and 180 m/s) to the constant bedrock V_s equal to 800 m/s. This latter assumption does not affect the validity of the parametric study provided that the prominent role of the velocity contrast or the impedance contrast on the valley amplification effects (see paragraph 2).

The sediment V_s values have been measured during the VEL project (Signanini et al. 2001; Rainone 2003; Foti and Lo Presti 2002; Lo Presti et al. 2007a,b) and reported in Table 3. Dynamic properties considered for the equivalent linear seismic soil behaviour are the curves of the shear modulus reduction $G(\gamma)/G_{max}$ and the damping ratio $D(\gamma)$, plotted in Fig. 5: these curves have been measured by resonant column tests (Lo Presti et al. 2007b) within the VEL project experimental activities. The initial values for the dynamic shear modulus G_{max} is drawn from the expression:

$$G_{max} = \rho \cdot V_s^2 \tag{2}$$

where V_s and ρ are the values reported in Table 4. Constant V_s values for surficial deposits over the first 30 m depth have been measured from field tests (Down hole, seismic refraction and reflection tests) within the Tuscan territory. Furthermore, the equivalent linear constitutive law used within numerical analyses have been tested to be adequate for seismic response description of Tuscan soils. The test consisted on checking the maximum strain values induced by seismic shaking: they show to be lower than the volumetric threshold according to each soil curves plotted in Fig. 5. The testing results show the suitability of the equivalent-linear behaviour for the considered Tuscan soils.

At the bottom of each valley model, a 5 m bedrock layer has been inserted in order to do the de-convolution of the input signal toward a horizontal base. Thereby, each model has the maximum soil thickness of 30 m at the centre of the valley with 5 m bedrock (Fig. 4b). Moreover, results have been calculated, in terms of acceleration spectra, at three points on the valley surface (Fig. 4b): at the centre (P1), at the edge (P3) and in between (P2).

2D numerical analyses have been performed by means of QUAKE/W (Krahn 2004). Triangular shaped elements have been used in the finite element domain discretisation. The optimum maximum size of the finite elements has been derived from the following rule, after Kuhlemeyer and Lysmer (1973):

$$l_{\max} = \frac{V_S}{7 \cdot f_{\max}} \quad (3)$$

where V_S is the shear wave velocity of the element material and f_{\max} is the maximum frequency value of the input signal to be propagated towards the surface, which is assumed to be 20 Hz. Boundary conditions applied to lateral cut-off boundaries are nodal zero vertical displacements for all the models and additional nodal horizontal dampers, for the case of $SR = 0.8$, with a viscosity coefficient, D_{node} , the values of which have been derived from the following relationship:

$$D_{\text{node}} = \rho V_S \cdot L/2 \cdot 1 \quad (4)$$

where ρ is the density and V_S is the shear wave velocity of the material, and $L/2$ is half the distance between the nodes times a unit distance into the section. These lateral boundary conditions are able to reduce the fictitious energy trapping within numerical simulations. Further details on preliminary benchmark activity on the valley models have been reported in Vessia et al. (2011). The maximum horizontal extension of the models varies according to the SR values, that is the slope chosen for the valley edges. Two types of boundary conditions have been applied at the base of the valley models: zero horizontal and vertical nodal displacements and nodal horizontal accelerations.

6 Input signals for 2D numerical simulations

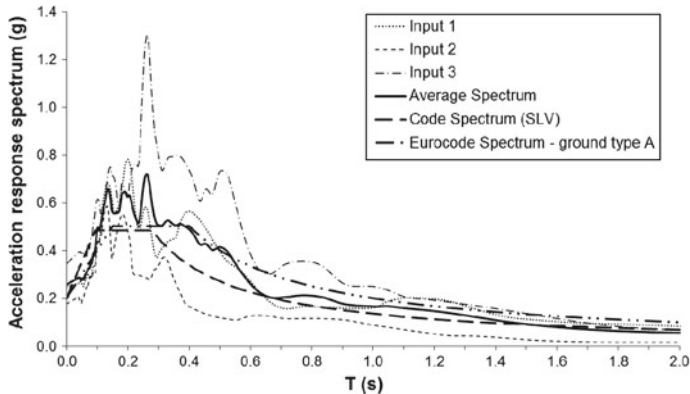
REXEL v 2.61 beta code has been used (Iervolino and Galasso 2010) to select the input accelerograms, in terms of horizontal components, among the Italian and European accelerometric databases. The choice of the range of periods is related to the most dangerous range of periods for buildings according to the purpose of this study. Such input signals were chosen to respect the spectrum-compatibility in the range of periods 0.1–2.0 s, that is the most affecting range of periods for buildings. The seismic-compatibility has been assessed by Lai et al. (2005), who performed a de-aggregation study of the seismic hazard in Garfagnana and Lunigiana territories. For this de-aggregation, couples of magnitude and distances ranging between 5.0 and 6.5 for the magnitude and between 5 and 20 km for the epicentral distances have been considered.

The reference spectrum for the spectrum compatibility of the chosen accelerograms is built according to EC8, by means of the national technical provision requirements: for the case studied it is the Italian building code (DM 14 gennaio 2008). Furthermore, the reference spectrum is compliant with the following assumptions: (1) the limit state is the ultimate limit of life safeguard (SLV), (2) building life (V_N) equals to 50 years, (3) the usage coefficient of the building (C_U) equals to 1 and (4) soil category is A with flat topographic surface (T1 is the topographic category). The reference site for studied seismic zone is assumed Castelnuovo Garfagnana city site and the maximum expected ground acceleration a_g is taken equal to 0.25 g, that is the maximum expected ground acceleration within seismic zone 2 (OPCM 2003).

In this study, three accelerograms out of seven retrieved by REXEL procedure have been used, whose spectrum-compatibility has been verified over the period range 0.1–2.0 s. The

Table 5 Main features of the three input signals used within the present numerical simulations

Waveform ID	Earthquake ID	Station ID	Earthquake name	Date	Mw	Epicentral distance (km)
258	69	PTL	Gubbio Earthquake	29/04/1984	5,6	26,1323
103	28	SRC0	Friuli Earthquake 4th Shock	15/09/1976	5,9	16,4207
14	4	TLM1	Friuli Earthquake 1st Shock	06/05/1976	6,4	21,7205

**Fig. 6** Acceleration response spectra of the three input signals recorded on soil A (Eurocode 8) and building code one for the ultimate limit state SLV

limited number of accelerograms do not affect the significance of results provided that a broad range of period content have been investigated with the chosen accelerograms, as stated by Chávez-García and Faccioli (2000). Moreover, according to past local seismic effect studies (Beyer and Bommer 2007) and EC8 (CEN 2003 par. 3.2.3.1.3), whenever seven accelerograms have been used, mean response spectral ordinates should be considered to estimate the design spectra, whereas when three accelerograms are considered the maximum spectral ordinates shall be taken into account. Thus, in this study, the maximum acceleration spectral ordinates have been calculated.

Main features of the chosen horizontal input records are summarized in Table 5 and their acceleration spectra are plotted in Fig. 6. Here, SLV spectrum, EC 8 spectrum and the input motion mean spectrum are plotted in order to show their spectrum-compatibility. In order to carry out 2D simulations, the input accelerograms were de-convolved from the surface to the bedrock at 35 m depth by means of EERA code, that simulates 1D propagation of in-plane shear waves throughout a layered subsoil by equivalent-linear analysis in the frequency domain (Bardet et al. 2000). The influence of input signal directivity on the seismic response of valley models has not been investigated because goes beyond the scope of the paper, that is the prediction of basin amplification effects due to horizontal input components.

7 Discussion on results

Results from 2D numerical analyses have been plotted in terms of maximum amplification functions A_v in Figs. 7, 8, 9, and 10a–c. The plotted A_v have been calculated for

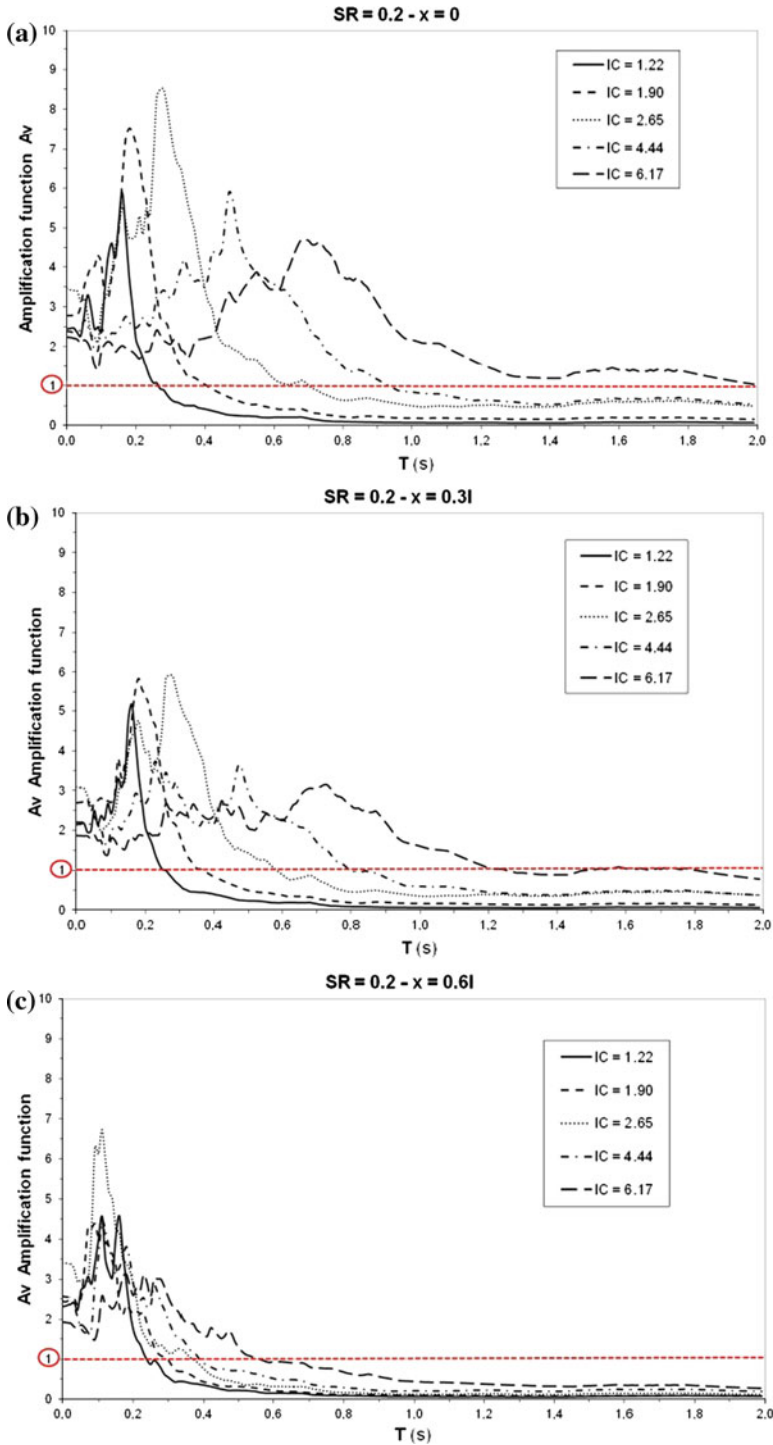


Fig. 7 Amplification functions calculated for $SR = 0.2$ at three locations on the surface: **a** at the centre; **b** at $x = 0.31$ and **c** nearby the edge $x = 0.61$

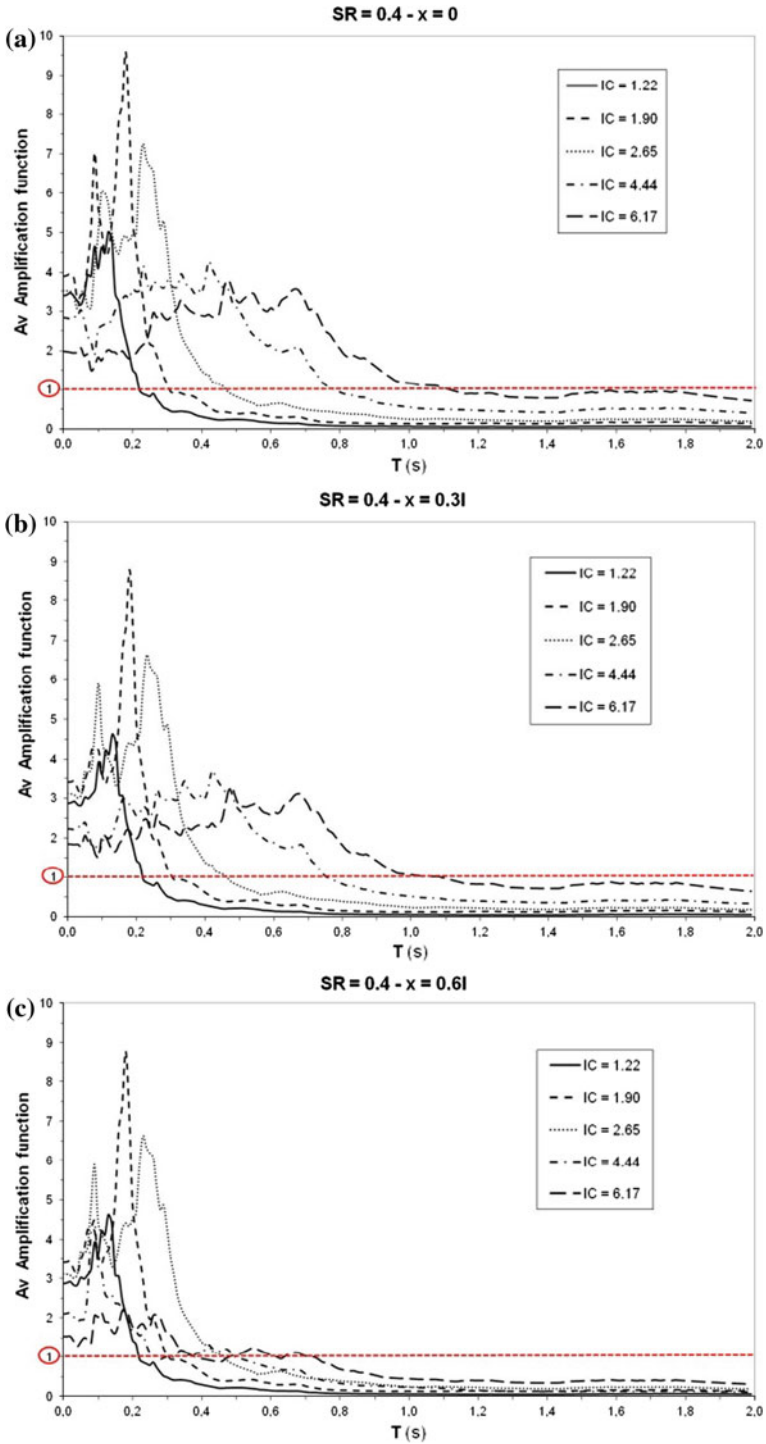


Fig. 8 Amplification functions calculated for SR = 0.4 at three locations on the surface: **a** at the centre; **b** at x = 0.31 and **c** nearby the edge x = 0.61

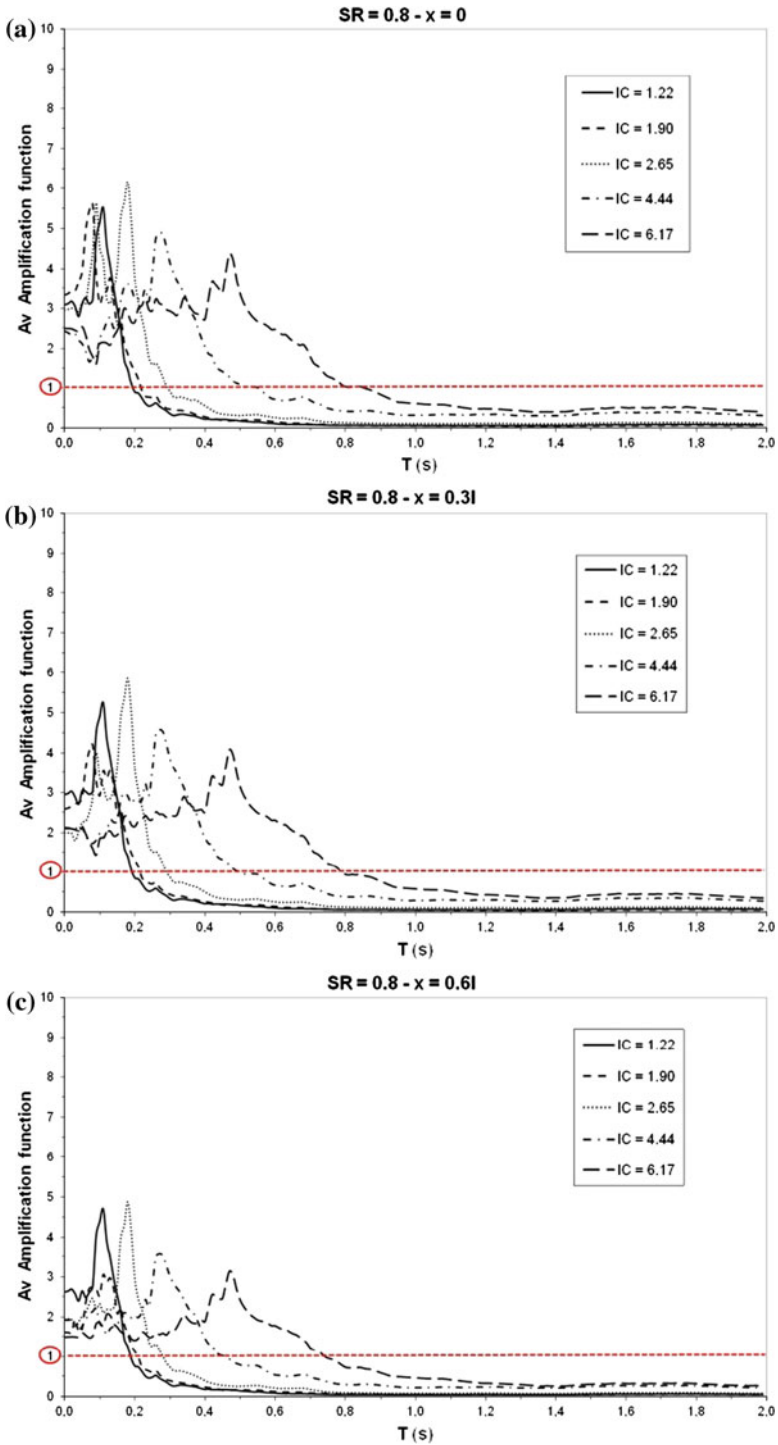


Fig. 9 Maximum amplification functions calculated for SR = 0.6 at three locations on the surface: **a** at the centre; **b** at x = 0.31 and **c** nearby the edge x = 0.61

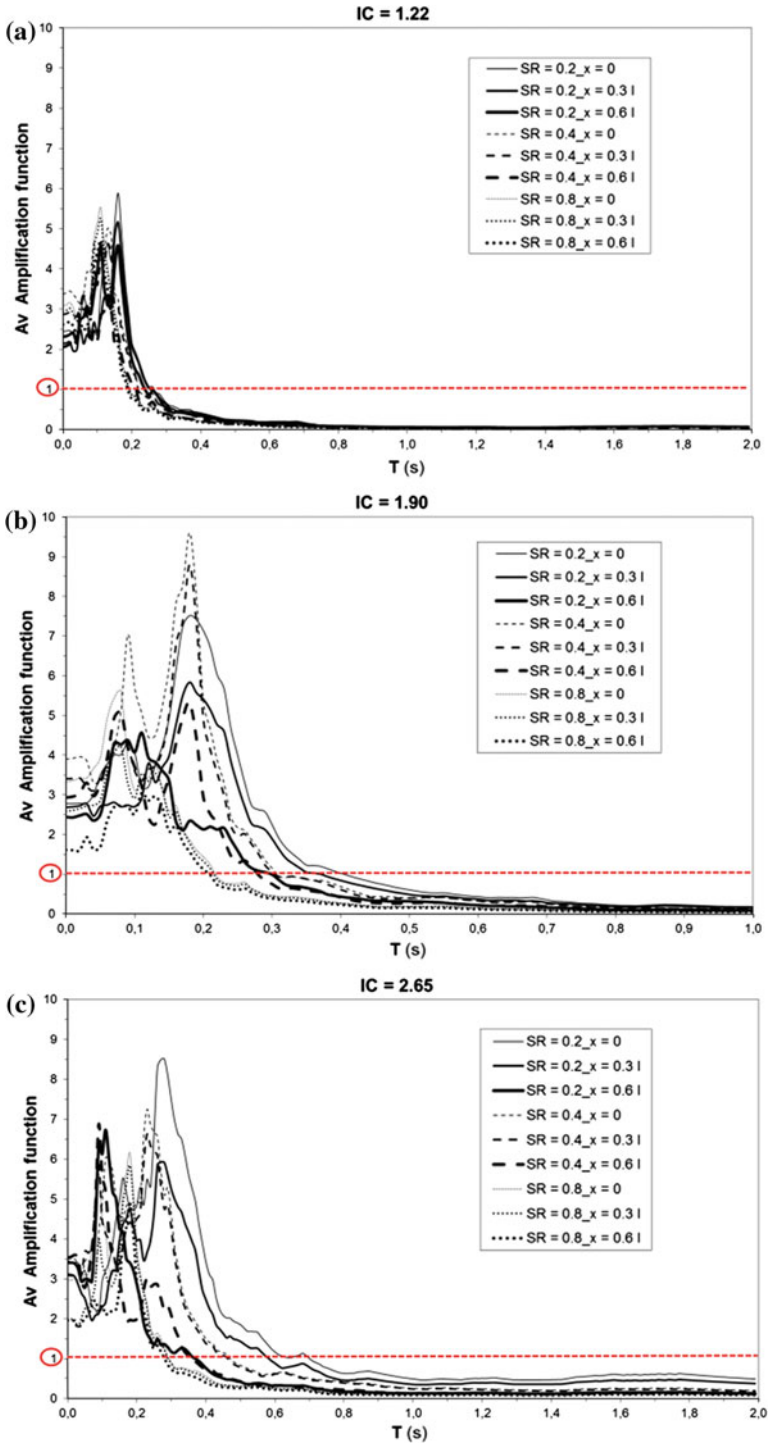


Fig. 10 Maximum amplification functions A_V calculated with respect to the impedance contrast values: **a–c** B soils; **d–e** C soils according to Eurocode 8

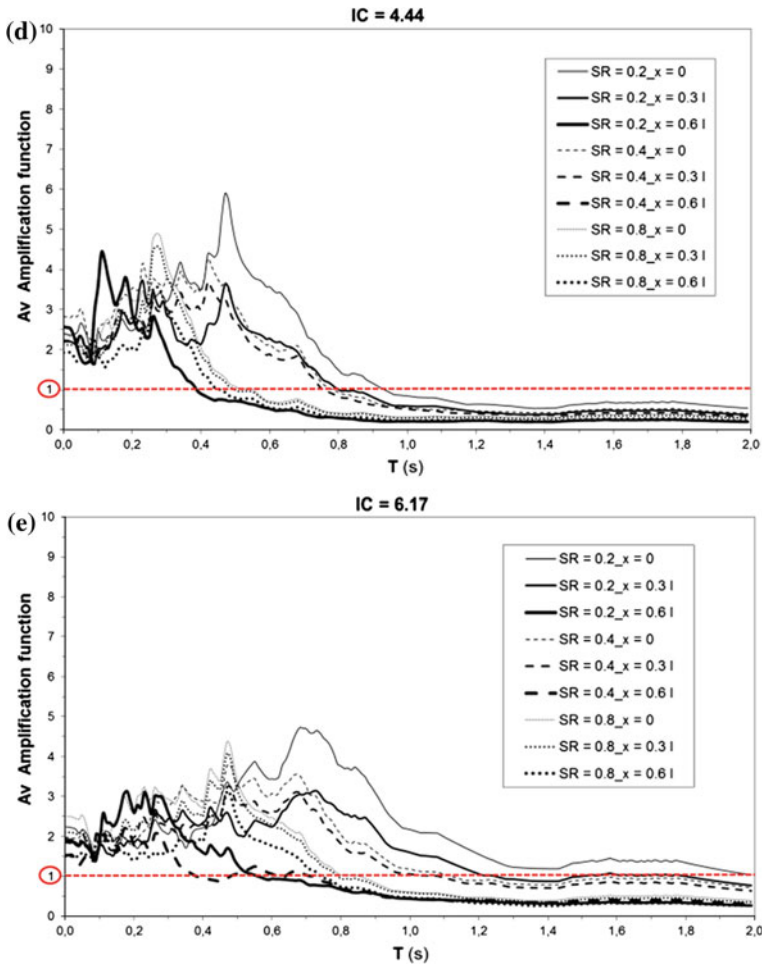


Fig. 10 continued

the three input motions considered (Table 5) and then the maximum values over the three spectral accelerations have been carried out for each period. A_v is obtained from the ratio between the valley surficial spectral acceleration at a point and the input spectral acceleration de-convoluted at the bottom of the valley model calculated over the range period 0.1–2.0 s. A_v has been calculated for three valley shapes (that are SR = 0.2, 0.4 and 0.8) and for five V_S values ranging between 780 and 180 m/s: such V_S values are reported in terms of five values of IC (Table 4). Moreover, three locations have been considered for calculating the seismic response (Fig. 4b): at the centre of the valley (where $x = 0$); between the centre and the edge of the valley (where $x = 0.31$) and near the valley edges (where $x = 0.61$). For each one of the abovementioned location, the A_v maximum values over the range period 0.1–2.0 s relating to the three input signals have been plotted in Figs. 7, 8, and 9 with respect to SR values (Fig. 7a–c for shallow valley, SR = 0.2; Fig. 8a–c for deep valley, SR = 0.4; Fig. 9a–c for very deep valley, SR = 0.8) and in Fig. 10a–e with respect to IC values.

Figure 7a–c shows A_v values decreasing from the centre toward the edges of the valley whereas the range of amplified periods reduces. As a matter of fact, the amplified period range at the centre is 0.05–2.0 s whereas at the edge, it reduces to 0.05–0.6 s. Correspondingly, the maximum amplifications of spectral accelerations at the centre (Fig. 7a) vary between 5 and 9 whereas at the edges between 3 and 4.5 for IC values 1.22, 1.90, 4.44 and 6.17. On the contrary, IC = 2.65 shows the maximum amplification at the centre of the valley, then it reduces at $x = 0.31$ then increases at the edge, at $x = 0.61$. According to the method used for plotting A_v such result corresponding to SR = 0.2 and IC = 2.65 can be due to the resonance effect of the input motion frequency content and the basin characteristic frequency. As a matter of fact, this difference in amplification trend between the two points 0.31 and 0.61 does not affect SR = 0.4 and 0.8. In the cases of deep valleys, on the contrary, both A_v peaks and the range of amplified periods slightly vary from the centre toward the edges of the valley (see Figs. 8, 9a–c): for SR = 0.4, the maximum A_v reduces from 9.5 at the centre to 9 at the edges whereas for SR = 0.8, A_v shows the same range of amplified periods and spectral peaks at each location on the surface.

In Fig. 10a–e, the three maximum valley responses in terms of A_v maximum function over the three input signals at each locations are grouped by IC values. The A_v trend shows high dependency on IC values so that it cannot be generalized. Accordingly, for the value IC = 1.22, A_v trend at the three points on the valley surface and for the three SR values are similar as both the range of periods and the amplification peaks are concerned. It is worth noticing that, in this case, the range of amplified periods is narrow (0.05–0.2 s) and the maximum A_v ordinates range between 5.5 and 6. As far as IC value increases, the amplified range of periods accordingly widens: for IC = 1.9, it is 0.05–0.4 s; for IC = 2.65, it is 0.05–0.7 s; for IC = 4.44, it is 0.05–0.9; for IC = 6.17, it is 0.05–2.0 s. On the other hand, when focusing on the A_v peaks, it can be seen that except for IC = 1.22 (that shows A_v maxima ranging between 4.5 and 6 within a low period range 0.1–0.2 s), from IC = 1.9 to 6.17, the A_v peak values decrease from 9.8 for IC = 1.9 (Fig. 10b) to 5 for IC = 6.17 (Fig. 10e). These outcomes are due to the complex multiple reflections of the waves on the valley boundaries. In a simple way, Fig. 11a–d shows the geometrical interactions among the incoming, refracted and reflected shear wave rays for the three valley models. It is a simplified representation of the Snell law:

$$n_1 \sin(\vartheta_1) = n_2 \sin(\vartheta_2) \quad (5)$$

Such expression controls the inclination of the reflected and refracted wave rays within the particular geometries of the three valley models: whenever $\theta_1 = 0^\circ$ than the angle of refraction is always $\theta_2 = 0^\circ$ whatever values are n_1 and n_2 . This means that the orthogonal wave ray to the interface is never deviated from the normal direction. The refraction indexes n_1 and n_2 for the case of shear wave ray are the shear wave velocities within the two materials: V_{S1} and V_{S2} .

Such representation can figure out the influence of the basin shape on the horizontal shear wave focalization throughout the valley surface in a simple but efficient fashion: Fig. 11a–c shows that within shallow valleys (SR lower than 0.2), the refracted shear waves are locally focalized toward the centre of the valley causing concentrated amplification. The inclination of the refracted wave ray depends on the IC value according to the Snell law (Eq. 5), that means the greater IC value the less the refracted ray inclination to the normal of the valley side. Thus, in the case of the shallow valley, higher IC values produce higher amplifications (due to the most of the energy trapped within the valley) but concentrated on a narrow part of the surface whereas lower IC values cause lower amplifications but spread out over the surface. Such spreading depends on the inclination of the valley side: as the valley gets deeper (SR greater than 0.2) the refracted rays are focused on a large part of the valley surface

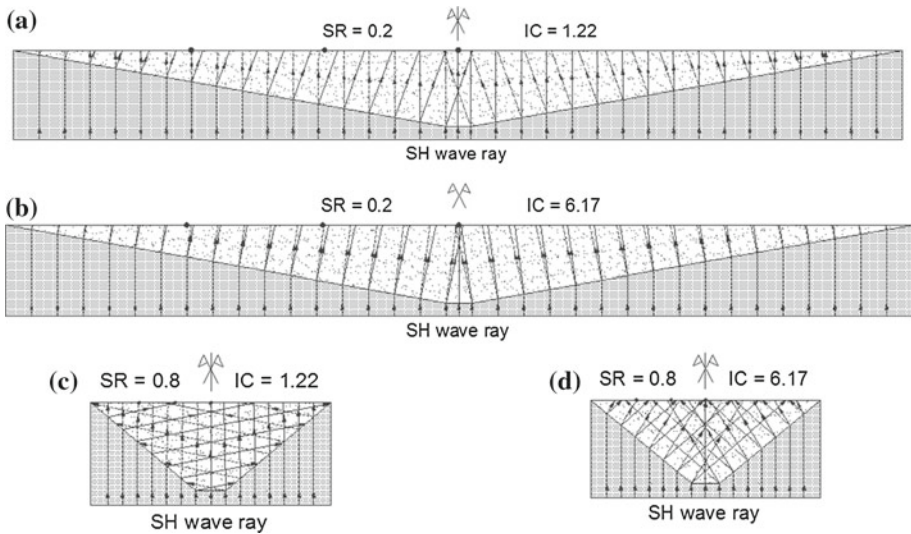


Fig. 11 Sketches of the horizontal shear wave rays at the bottom of the valley models and within the basins, where they interact according to Snell law refraction: **a** SR = 0.2, IC = 1.22; **b** SR = 0.2, IC = 6.17; **c** SR = 0.8, IC = 1.22; **d** SR = 0.8, IC = 6.17

(see Fig. 11c, d). In the cases of deep valleys, differences between seismic response at the centre of the valley and at the edges are almost negligible. The focalization depends on the basin curvature, that can be interpreted by SR only in few cases, and on the velocity contrast between the sediments and the basin.

As the sediment impedance contrasts are concerned, Fig. 10b–c show that the most amplified IC values range between 1.90 and 2.65. This means, according to EC8 seismic soil categories, that soil B is the most amplified. Such result can be related to the damping and shear modulus curves measured (Fig. 5): the damping curve of soil B always lies below the curve of soil C meaning that soil C should be less amplified than soil B.

8 The estimation of valley effects by means of the “valley effect charts”

The present numerical analyses are aimed at calculating amplification indexes for taking into account the “valley amplification effects” within microzoning studies. This amplification factor can be used for estimating the surface maximum acceleration value, that is the PGA at a site. Such value is useful for defining the design spectra according to building code (e.g. EC8).

Accordingly, three “valley effect charts” have been plotted in Fig. 12a–c to be applied to three homogeneous amplification areas corresponding to three parts of the urban centre placed on a sediment filled basins: at the centre, at the edge and in between along the valley width. In these figures, the discussed results (Figs. 7, 8, 9a–c) have been plotted as a new amplification factor F_A . F_A values have been calculated as follows:

$$F_A = \frac{\int_{i=0.05}^{2.0} \max(A_v)_i dt}{\Delta T} \tag{6}$$

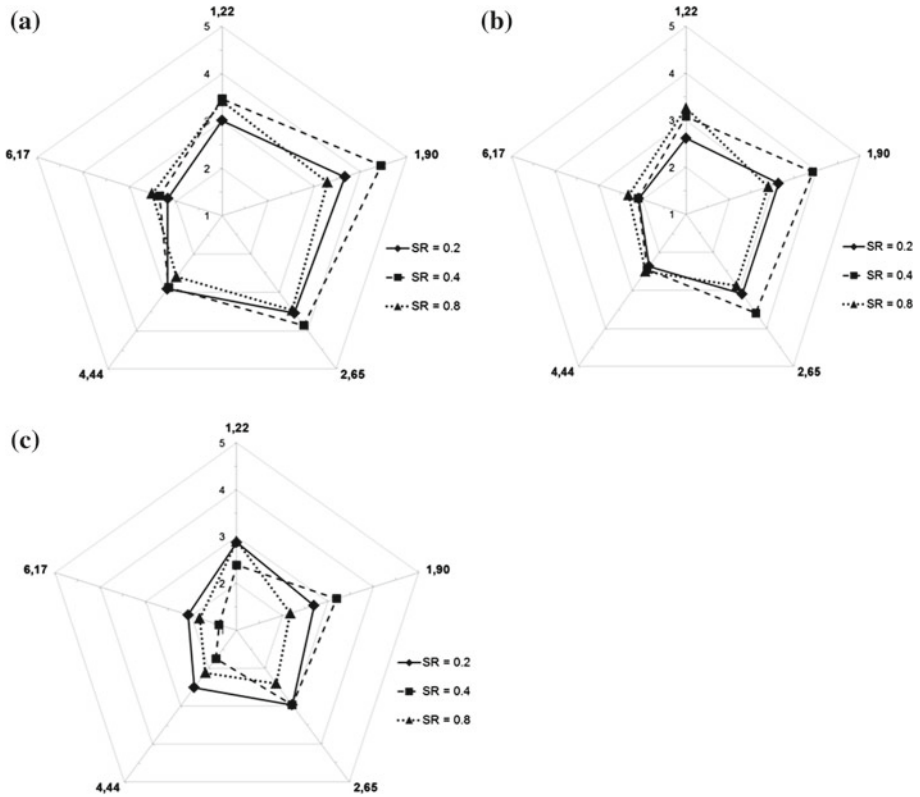


Fig. 12 Valley effect charts proposed for estimating local seismic amplification, calculated for the three points on the surface (see Fig. 4b): **a** P1 ($x = 0$); **b** P2 ($x = 0.31$) and **c** P3 ($x = 0.61$)

where $\max(A_v)$ is the maximum values of the amplification function higher than one, for the three input signals calculated over the corresponding period range varying between 0.05 and 2.0 s, and ΔT is the considered period range, whose maximum value is $\Delta T = (2.0 - 0.05)s$. Thus, 15 F_A values have been calculated corresponding to IC and SR investigated values. Three graphs are proposed for the three studied locations over the valley surface, that are the centre (Fig. 12a), the edge (Fig. 12c) and the point in between (Fig. 12b). Such positions represent three different points within the urban centres placed on a sediment filled valley that have been affected by different amplification values. In each radar graph, at the vertices can be seen the IC values. F_A values reported on IC axes are joint by three types of lines referring to the three SR values: pointed line with triangle for SR = 0.8, dotted with quadrangle for SR = 0.4 and solid with diamond for SR = 0.2. Each IC axes show F_A values ranging from 1 to 5; thus F_A values, that are A_v integral values, increase from 1 (that means no amplification) to 5 (that means, the surface response is 5 times the input signal).

At the center of the valley, Fig. 12a shows the highest value of $F_A = 4.5$ for SR = 0.4 and IC = 1.9. This means that a deep valley, but not the deepest, shows the highest comprehensive amplification value of 4.5 for low impedance ratio: in the cases studied, the most dangerous combination is SR = 0.4 and IC = 1.9 at the center of the valley. This is also true at $x = 0.31$ and $x = 0.61$ on the valley surface, where $F_A = 4$ and 3.2, respectively. Furthermore, from the center toward the edges F_A values reduce (compare Fig. 12a with b and Fig. 12a with c).

Moreover, the most amplified shape ratio is 0.8 for IC ranging from 4.44 to 6.17 at $x = 0.31$ with $F_A = 2.5$; whereas it is 0.2 for $x = 0.61$ with $F_A = 2.5$. At the center, for the same IC range, $F_A = 2.5$ for IC = 6.17 and SR = 0.8; while $F_A = 3$ for IC = 4.44 and SR = 0.2.

These results confirm the findings of previous studies about the relevant edge amplification for shallow valley cases and the amplification spread out over the deep valley surface. Moreover, the relevant role of IC on amplification effects within sediment filled valleys has been evidenced by means of the Fig. 10 according to literature studies (Faccioli and Vanini 1998; Makra et al. 2005; Vanini et al. 2007). Numerical simulation results show a high influence of input motions on the valley surface response that is confirmed by past experimental evidences (King and Tucker 1984; Tucker and King 1984). The correspondence between the present numerical results relating to Tuscan Region conditions investigated by means of IC and SR parameters and the experimental ones performed worldwide enables these results to be applied where similar IC and SR values can be measured.

Additionally, when equivalent-linear soil behavior and real input signals are considered, the maximum amplification values are attained for particular combinations of IC and SR values that cannot be predicted in advance by means of simplified wave propagation studies with assumed constant damping for visco-elastic behavior of sediments filling the basins. Finally, the importance of IC upon SR for amplification values at the center of the valley is here confirmed. Further experimental studies are needed for investigating the inefficiency of the shape ratio in describing the basin geometry and relating it to the wave focalization within the basins.

9 Discussion on the application of the valley effect charts to design spectra

The aforementioned three charts, related to the three SR and the five IC values investigated, show that over the whole surface of a valley width (at the center, at the edge and in between) the amplifications cannot be neglected. According to these results, the authors suggest to directly apply the F_A to the EC8 design spectrum (type I, that is used for expected surface wave Magnitude higher than 5.5 earthquake), according to the soil type (that is IC) and the valley type (that is SR). As a matter of fact, the EC8 defines the shape of the design spectrum as shown in Fig. 13a, where S is the amplification factor depending on the soil type, s_g is the design ground acceleration on type A ground (rock type) and η is the damping correction factor with a reference value of $\eta = 1$ for 5% viscous damping. Figure 13b plots type I design

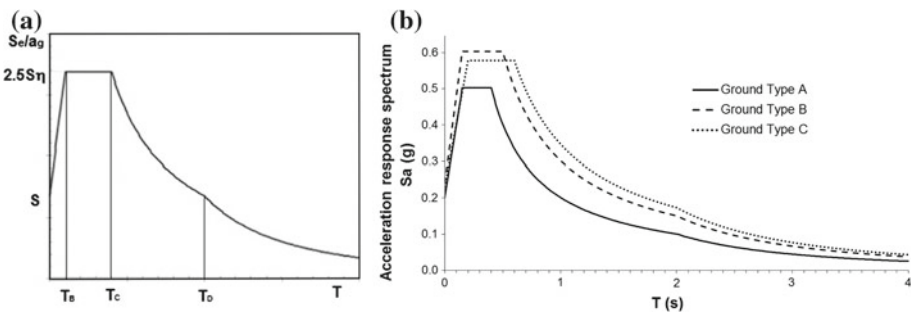


Fig. 13 a Shape of the elastic response spectrum according to EC 8; b EC8 type I design spectrum for soil type A, B and C with $a_g = 0.201g$

Table 6 Values of the parameters describing the recommended elastic response spectra when bedrock basin shaped are filled with B and C seismic ground type

Ground type	IC	SR						T_B (s)	T_D (s)
		0.2		0.4		0.8			
		F_A	T_C (s)	F_A	T_C (s)	F_A	T_C (s)		
B	1.22	3.0	0.4	3.43	0.3	3.43	0.2	0.05	2.0
	1.9	3.66	0.4	4.45	0.3	4.45	0.2	0.05	2.0
	2.65	3.46	0.4	3.87	0.3	3.87	0.2	0.05	2.0
C	4.44	2.87	0.7	2.87	0.6	2.6	0.6	0.2	2.0
	6.17	2.17	0.7	2.35	0.6	2.52	0.6	0.2	2.0

spectrum modified for three soil type: A, B and C and related to $a_g = 0.201g$ according to the studied site reference acceleration. Thus, when basin shaped bedrock is detected, this study proposes to change the perspective: the soil type is replaced by the impedance contrast (IC) and introduces the shape ratio (SR). Accordingly, the EC8 spectra will be modified by means of F_A values summarized in Table 6. Table 6 shows the calculated F_A that will be multiplied to the spectrum ordinates for modifying it, as shown in Fig. 14a, b. These figures relate to the case of a point placed at the center of the valley with $SR = 0.4$. As Fig. 14 point out, the two EC 8 design spectra for B (Fig. 14a) and C (Fig. 14b) soil types are inadequate for taking into account the valley effects according to the wave trapping phenomenon. On the contrary, F_A reasonably increases the maxima ordinates of these design spectra varying according to the IC values. IC values have large ranges of variation within B or C soils; thus, when filled basin shaped bedrocks are detected the “seismic soil type” can be not adequate for estimating the local amplifications.

Moreover, from the present study, the three periods needed for building the design spectrum by EC 8 (Fig. 13a) can be taken from Table 6 (columns 4, 6, 8 and 9): it is worth noticing that for all of the IC values corresponding to soil B, T_B is 0.05 s whereas it is 0.2 for those values corresponding to soil C. On the contrary, T_C strictly depends on the IC values and it changes as shown in Table 6. Figure 14 again put in evidence that valley effects cause wider amplified ranges of periods for both stiffer and softer soils. These ranges include both higher and lower periods than those considered by EC 8, type I (Fig. 13b).

10 Conclusions

This paper illustrates a numerical investigation of “valley amplification effects” within Tuscan region territories and proposes an index of local seismic amplification. It is called F_A and it has calculated for three valley shapes: shallow with $SR = 0.2$ and deep valleys: $SR = 0.4$ and 0.8 . Moreover, real sediment behaviour under seismic loading has been employed within numerical simulations, five IC values have been considered and three input motions from Italian strong motion registration database have been applied. The present results confirm some outcomes already shown by literature, that can be summarized below:

1. At the centre and at the edges of a shallow basin the amplifications on the surface cannot be neglected even in the case of low IC values;

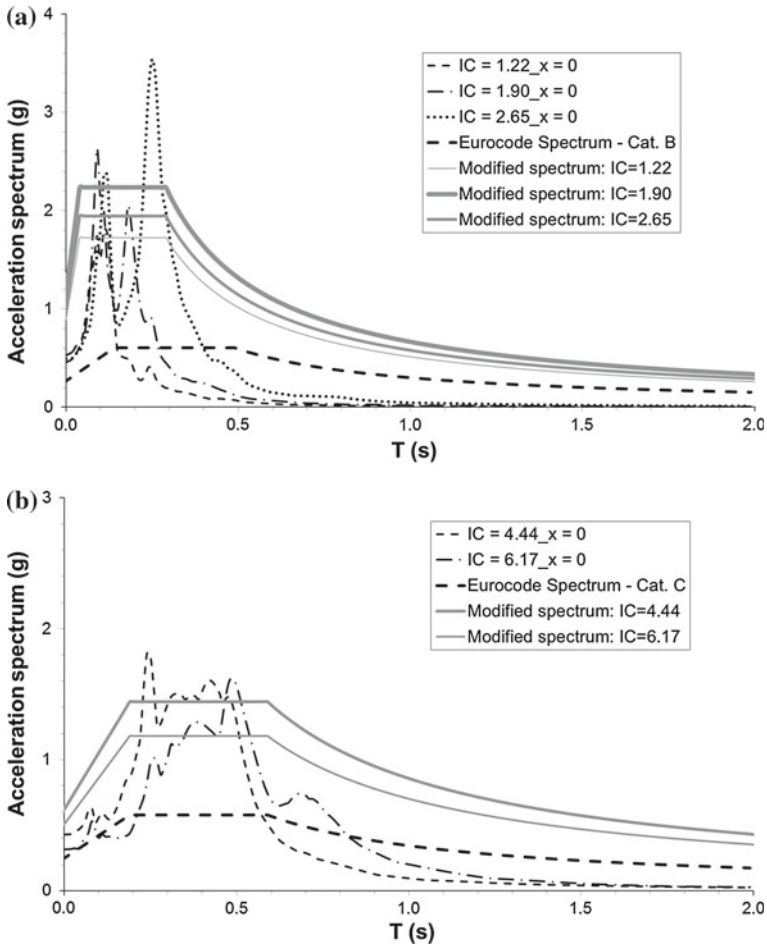


Fig. 14 Design spectra for $SR = 0.4$ according to EC 8 and modified by means of F_A from the present study, for two soil types: **a** B and **b** C and five IC values

2. The maximum amplification magnitude depends on IC and SR values although SR seems not to be able to completely describe the possible complex geometries.

Furthermore, some novel outcomes have shown by means of the proposed amplification factor F_A :

3. At the edge of the valleys, the most amplified valley model ($F_A = 3.2$) is the deep valley $SR = 0.4$ and $IC = 1.9$. Such IC values correspond to sediments classified as B soil according to EC8. At the edge, the shallow valley, that is $SR = 0.2$, shows the highest amplification values for the remainder IC values.
4. At the centre of the valley, B soil is the most amplified case when $SR = 0.4$. The reason for such result is provided into the previous paragraphs and can be understood by considering the refracted wave ray inclinations (depending on IC values and the basin edge inclination) and the damping and stiffness reduction functions characteristics of dynamic behaviour of B and C soils.

Finally, the proposed amplification “charts” can be used for microzoning studies when basin effects shall be taken into account, provided that sediments filling the basins belong to B and C seismic soil categories with dynamic behaviour similar to the studied sediments and the basin geometries have the same characters of the Tuscan ones. Moreover, the amplification factors F_A from these charts can be applied directly to EC8 design spectra provided that, SR and IC values are used for instead of seismic soil types and amplification factor S for building the spectrum.

References

- AAVV (2004) Guide Geologiche Regionali. Appennino Tosco-Emiliano. BE-MA, Firenze
- Barchi M, Landuzzi A, Minelli G, Piali G (2001) Outer Northern Apennines. In: Vai GB, Martini IP (eds) Anatomy of an orogen. The Apennines and adjacent Mediterranean Basins. Kluwer Academic Publishers, Great Britain, pp 215–254
- Bard PY, Bouchon M (1980a) The seismic response of sediment-filled valleys. Part I. The case of incident SH waves. *Bull Seismol Soc Am* 70:1263–1286
- Bard PY, Bouchon M (1980b) The seismic response of sediment-filled valleys. Part II. The case of incident P and SV waves. *Bull Seismol Soc Am* 70:1921–1941
- Bard PY, Bouchon M (1985) The two-dimensional resonance of sediment-filled valleys. *Bull Seismol Soc Am* 75(2):519–541
- Bardet JP, Ichii K, Lin CH (2000) EERA: a computer program for equivalent-linear earthquake site response analyses of layered soil deposits. University of Southern California, Department of Civil Engineering
- Bartolini C (2001) When did the Northern Apennine become a mountain chain? *Quat Int* 101:75–80
- Benvenuti M (1995) Il controllo strutturale nei bacini intermontani plio-pleistocenici dell'Appennino settentrionale: l'esempio della successione fluvio-lacustre del Mugello (Firenze). *Il Quaternario* 8:53–60
- Beyer K, Bommer JJ (2007) Selection and scaling of real accelerograms for bi-directional loading: a review of current practice and code provisions. *J Earthq Engi* 11:13–45
- Bielak J, Xu J, Ghattas O (1999) Earthquake ground motion and structural response in alluvial valleys. *J Geotech Geoenviron Engi* 125(5):413–423
- Bosi C, Messina P, Moro M (2004) Quaternary geological map of the upper Aterno valley (Central Italy). In Pasquarè G and Venturini C (Ed) Mapping geology in Italy, 32nd International Geological Congress (32IGC), Florence, Italy pp 20–28
- Bossio A, Costantini A, Lazzarotto A, Liotta D, Mazzanti R, Mazzei R, Salvatorini G, Sandrelli F (1993) Rassegna delle conoscenze sulla stratigrafia del neoaotoceno toscano. *Memorie della Società Geologica Italiana* 49:17–97
- Castro RR, Pacor F, Bindi D, Franceschina G, Luzi L (2004) Site response of strong motion stations in the Umbria region, Central Italy. *Bull Seismol Soc Am* 94:576–590
- Cauzzi C, Faccioli E, Costa G (2010) 1D and 2D site amplification effects at Tarcento (Friuli, NE Italy), 30 years later. *J Seismol*, doi:10.1007/s10950-010-9202-y
- Chávez-García FJ, Faccioli E (2000) Complex site effects and building codes: making the leap. *J Seimol* 4:23–40
- CEN (2003) “Eurocode 8: design of structures for earthquake resistance. Part. 1: General rules, seismic actions and rules for buildings
- CNR-PFG (1987) Neotectonic Map of Italy. *Quaderni de la Ricerca Scientifica* 114
- D'Amato G, De Lucia PL, Nardi R, Pochini A, Puccinelli A, Trivellino M (1986) Carta geologica e Carta della Franosità della Garfagnana e della Valle del Serchio (Lucca) in scala 1:10.000, tipografia SELCA
- Day SM, Bielak J, Dreger D, Graves R, Larsen S, Olse KB, Pitarka A, and Ramirez-Guzman L (2006) Numerical simulation of basin effects on long-period ground motion. In: 8th National Conference of Earthquake Engineering, San Francisco, pp 18–22
- Delgado J, Faccioli E, Paolucci R (2001) Influence of complex amplification effects on ground motion: the case of an alpine valley in Northern Italy. In: Faccioli P (ed) CAFEEL-ECOEST2/CONS Report 1, LNEC, Lisbon, “Seismic Action”
- DM 14 gennaio (2008) Norme Tecniche per le Costruzioni. G.U. n. 29 del 4 febbraio 2008
- Faccioli E, Vanini M (1998) Studio della risposta sismica locale nella zona di Trento Nord. Technical Report for the Autonomous Province of Trento, Italy (in italian)
- Faccioli E, Vanini M (2003) Complex seismic site effects in sediment-filled valleys and implications on design spectra. *Earthq Engi struct dyn* 5:223–238

- Foti S, Lo Presti D, Pallara O, Rainone ML, Signanini P (2002) Indagini geotecniche e geofisiche per la caratterizzazione del sito di Castelnuovo Garfagnana (Lucca). *Rivista Geotecnica Italiana* 3:42–60
- Gazetas G (1997) Contribution of National Technical University of Athens (Soil Mechanics and Soil Dynamics Laboratory). In: Faccioli E (ed) *TRISEE—3D Site Effects and Soil-Foundation Interaction in Earthquake and Vibration Risk Evaluation—First year Project report to the European Commission*. Environment and Climate Programme, Milan
- Gelagoti F, Gazetas G, Kourkoulis R (2007) 2D wave effects in alluvial valleys: how important and predictable are they?. In: 4th International Conference on Earthquake Geotechnical Engineering, Thessaloniki, Greece, pp 25–28
- Gruppo di lavoro CPTI (2004) Catalogo parametrico dei terremoti italiani, versione 2004 (CPTI04), INGV Bologna, <http://emidius.mi.ingv.it/CPTI04>
- Guidoboni E, Comastri A (2005), Catalogue of Earthquakes and tsunamis in the Mediterranean Area from the 11th to the 15th century. INGV-SGA, Bologna, 1037
- Iervolino I, Galasso C (2010) REXEL 2.61 beta - Computer aided code-based real record selection for seismic analysis of structures [v 2.61 beta - built 06/04/10]. Dipartimento di Ingegneria Strutturale, Università degli studi di Napoli Federico II. tutorial, available at: <http://www.reluis.it/doc/software/rexeltutorialeng.pdf>
- King JL, Tucker BE (1984) Observed variations of earthquake motion across a sediment-filled valley. *Bull Seismol Soc Am* 74(1):137–151
- Krahn J (2004) Dynamic modeling with Quake/W. Geoslope International Ltd, Calgary
- Kuhlemeyer L, Lysmer J (1973) Finite element method accuracy for wave propagation problems. *J Soil Mech Found Div* 99:421–427
- Lai C, Strobbia C, Dall'ara M (2005) Convenzione tra Regione Toscana e Eucentre. Parte 1. Definizione dell'Input Sismico per i Territori della Lunigiana e della Garfagnana. L.R. 56/97 programma VEL
- Lanzo G, Pagliaroli A (2009) Numerical modeling of site effects at San Giuliano di Puglia (southern Italy) during the 2002 molise seismic sequence. *J Geotech Geoenviron Eng* 135(9):1295–1313
- Lo Presti DC, Squeglia N, Baglione M, Ferrini M, Mensi E, Pallara O (2007a) Caratterizzazione meccanica dei depositi di terreni mediante prove penetrometriche dinamiche alla luce dei risultati acquisiti nell'ambito del progetto VEL della Regione Toscana. In 12simo Convegno L'Ingegneria Sismica in Italia. Pisa 1, pp 315–327
- Lo Presti DC, Squeglia N, Baglione M, Ferrini M, Mensi E, Pallara O (2007b) Caratterizzazione meccanica dei depositi di terreni mediante prove di laboratorio per l'analisi di risposta sismica alla luce dei risultati acquisiti nell'ambito del progetto VEL della Regione Toscana. In 12simo Convegno L'Ingegneria Sismica in Italia. Pisa, 1, pp. 302–314
- Luzi L, Bindi D, Franceschina G, Pacor F, Castro RR (2005) Geotechnical site characterisation in the Umbria Marche area and evaluation of Earthquake site-response. *Pure Appl Geophys* 162:2133–2161
- Makra K, Chavez-Garcia FJ, Raptakis D, Pitilakis K (2005) Parametric analysis of the seismic response of a 2D sedimentary valley: implications for code implementations of complex site effects. *Soil Dyn Earthq Eng* 25:303–315
- Mantovani E, Viti M, Babbucci D, Cenni N, Tamburelli C, Vannucchi A, Falciani F, Fianchisti G, Baglione M, D'intinosante V, Fabbroni P (2011) Sismotettonica dell'Appennino settentrionale. Implicazioni per la pericolosità sismica della Toscana. Centro stampa Giunta Regione Toscana
- Martini IP, Sagri M (1993) Tectono-sedimentary characteristics of Late Miocene-Quaternary extensional basins of the Northern Apennines, Italy. *Earth Sci Rev* 34:197–233
- Mariotti D, Guidoboni E (2006). Seven missing damaging earthquakes in Upper Valtiberina (Central Italy) in 16th-18th century: research strategies and historical sources. *Annals of Geophysics*, 49(6): 1139-1155
- Meletti C, Moretti A, Scandone P (1993) Schema sismotettonico del segmento appenninico compreso tra il Passo della Cisaie l'alta Val Tiberina. Dipartimento di Scienze della Terra, Università di Pisa, Internal report ENEL-CRIS, p 34
- Moretti A (1992) Evoluzione tettonica della Toscana settentrionale tra il Pliocene e l'Olocene. *Bollettino della Società Geologica Italiana* 111:459–492
- OPCM (Ordinanza del Presidente del Consiglio dei Ministri) n. 3274 del 20 marzo 2003 (2003) Primi elementi in materia di criteri generali per la classificazione sismica del territorio nazionale e di normative tecniche per le costruzioni in zona sismica. G.U. n. 72
- Paolucci R (1999) Shear resonance frequencies of alluvial valleys by Rayleigh's method. *Earthq Spectr* 15(3):503–521
- Paolucci R, Smerzini C (2011) 3D Numerical simulations of earthquake ground motion in sedimentary basins: the cases of Gubbio and l'Aquila, central Italy. 4th International Symposium IAEE, California, pp 23–26
- Psarropoulos PN, Gazetas G (2007) Effects of soil non linearity on the geomorphic aggravation of ground motion in alluvial valleys. In: 4th International Conference on Earthquake Geotechnical Engineering, Thessaloniki, Greece, pp 25–28

- Puglia R, Klin P, Pagliaroli A, Ladina C, Priolo E, Lanzo G, Silvestri F (2009) Analisi della risposta sismica locale a San Giuliano di Puglia con modelli 1D, 2D e 3D. *Rivista Italiana di Geotecnica* 63(3):62–71
- Rainone ML (2003) Istruzioni tecniche per le indagini geologico-tecniche, le indagini geofisiche e geotecniche, statiche e dinamiche, finalizzate alla valutazione degli effetti locali nei Comuni classificati sismici della Toscana. Direzione Generale Politiche Territoriali e Ambientali, Area Servizio Sismico Regionale
- Roten D, Cornou C, Steimen S, Fäh D, Giardini D (2004) 2D resonances in Alpine Valleys identified from ambient vibration wavefields. In: 13th World Conference on Earthquake engineering, Vancouver, B.C., Canada, pp 1–6
- Russo S, Vessia G, Cherubini C (2008) Considerations on different features of local seismic effect numerical simulations: the case studied of Castelnuovo Garfagnana. In: 6th International Conference on Case Histories in Geotechnical Engineering, Arlington, pp 11–16
- Silva WJ (1988) Soil response to earthquake ground motion. EPRI Report NP-5747. Electric Power Research Institute, Palo Alto, California
- Signanini P, Ferrini M, Rainone ML, D'Intinosante V (2001) Metodi geofisici integrati per la ricostruzione del sottosuolo e per la caratterizzazione dinamica dei terreni negli studi di microzonazione sismica: alcuni esempi relativi al Progetto VEL. Regione Toscana. In: Vol. Abstract of GEOITALIA FIST, settembre, Chieti, pp 4–7
- Tucker BE, King JL (1984) Dependence of sediment-filled valley response on input amplitude and valley properties. *Bull Seismol Soc Am* 74(1):153–165
- Vanini M, Pessina V, Di Giulio G, Lenti L (2007) Influence of alluvium filled basins and edge effect on displacement response spectra. Deliverable D19 of Project S5, available at <http://progetto5.stru.polimi.it>
- Vessia G, Russo S, Lo Presti D (2011) A new proposal for the evaluation of the amplification coefficient due to valley effects in the simplified local seismic response analyses. *Ital Geotech J* 4:51–77
- Zhang B, Papageorgiou AS (1996) Simulation of the response of the Marina District basin, San Francisco, California, to the 1989 Loma Prieta Earthquake. *Bull Seismol Soc Am* 86(5):1328–1400